

A Hybrid Fault Diagnosis Approach for Hydraulic Systems by using Radial basis Function Networks

Xiang-yu He^{1,2}, Yijiao Yang² and Shanghong He²

¹State Key Laboratory of Fluid Power Transmission and Control, Zhejiang University, Hangzhou, 310027, China

²Key Laboratory of Lightweight and Reliability Technology for Engineering Vehicle of Education Department of Hunan Province, Changsha University of Science and Technology, Changsha, Hunan, 410004 China
hexiangyu@hotmail.com

Abstract

To improve the reliability of hydraulic systems, a fault diagnosis approach based on radial basis function (RBF) networks was proposed in this paper. According to the target fault features extracted from a fuzzy auto-regressive with extra outputs (FARX) model, RBF networks serve as a fault classifier and the output of the RBF networks is the result of fault diagnosis. Several typical faults of hydraulic systems were used to test the fault diagnosis approach. Experiment results showed that the fault diagnosis approach is feasible and effective for improving the reliability of hydraulic systems.

Keywords: Hydraulic system, Fault diagnosis, Radial basis function neural networks, Fuzzy logic, Auto-regressive with extra outputs (ARX) model

1. Introduction

Faults in a hydraulic system can take many forms, such as pump faults, valve faults, and cylinder faults. Hydraulic faults are generally sorted in several grades according to severity. Complete failures and abrupt faults are comparatively easy to detect. Thus, fault detection techniques related to the complete failures of the control and equipment components of hydraulic systems have been proposed in previous studies. Gradually generating faults are difficult to detect early by limit-checking methods with simple residuals because fault effects are often masked by control actions. However, hydraulic systems are nonlinear with dynamic properties. Hence, classifying fault information on hydraulic systems by conventional techniques is difficult.

The main challenges of fault diagnosis are given by knowledge representation, prior knowledge introduction, typical symptom distributions, and data size. Classification methods are important in diagnosis, particularly if structural knowledge is unavailable for the relationship between symptoms and faults. Techniques based on artificial neural networks (ANNs) have an advantage over conventional techniques in significantly improving the accuracy of fault diagnosis because ANNs are capable of nonlinear mapping, parallel processing, and learning. These attributes make ANNs ideally suited for providing high accuracy in fault detection under a wide variety of systems and conditions.

Radial Basis function (RBF) networks emerged as a variant of ANNs in the late 1980's. However, the roots are entrenched in old pattern recognition techniques, such as potential functions, clustering, functional approximation, spline interpolation, and mixture models [1]. RBFs are embedded in a two-layer neural network where each hidden unit implements a radial activated function. The output units implement a weighted sum of hidden unit outputs.

The input for the RBF network is nonlinear whereas the output is linear. The excellent approximation capabilities have been studied in [2, 3]. RBF networks, which have nonlinear approximation properties, are capable of modeling complex mappings, whereas perceptron neural networks can only model complex mappings by multiple intermediary layers.

RBF networks have been successfully applied to various fields, such as interpolation, chaotic time-series modeling, system identification, control engineering, electronic device parameter modeling, channel equalization, speech recognition, image restoration, shape from shading, 3D object modeling, motion estimation, moving object segmentation, and data fusion [4-6].

In this study, a fault diagnosis approach based on RBF networks was proposed. First, a fuzzy auto-regressive with extra outputs (FARX) model was used to extract fault features. The FARX model obtains more accurate fault features of nonlinear characterizations than conventional auto-regressive with extra outputs (ARX) model [7-9]. RBF networks were trained with data under a variety of fault conditions and then used for fault type classification on the hydraulic system. This approach was effectively applied on an excavator hydraulic system and could accurately diagnose faults.

2. RBF Networks

RBFs are embedded into a two-layer feed forward neural network, which is characterized by a set of inputs and a set of outputs. A layer of processing units called hidden units is located between the inputs and outputs. Each of these hidden units implements an RBF. The manner in which the network is used for data modeling is different when estimating time-series and pattern classification. The structure of an RBF networks includes three layers, namely, the input layer, hidden layer, and output layer (Figure 1).

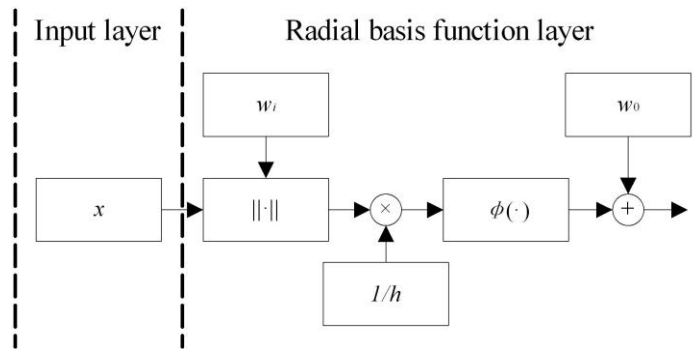


Figure 1. Structure of RBF Networks

To use RBF Networks, we need to specify the hidden unit activation function, the number of processing units, a criterion for modeling a given task, and a training algorithm for finding the network parameters. Finding the RBF weights is called network training. If we have a set of input-output pairs called training set, we can optimize the network parameters to fit the network outputs from the given inputs. The fit was evaluated by means of a cost function, which is usually assumed to be the mean square error. After training, the RBF network could be used with data that have underlying statistics similar to that of the training set. Online training algorithms adapt the network parameters to the changing data statistics.

An RBF network could be expressed as follows:

$$g(x) = \sum_{j=1}^k \omega_j \varphi \left(\frac{\|\mathbf{x} - \mathbf{c}_j\|}{h} \right), \quad (1)$$

where k is the number of basis function, $\mathbf{x} \in R^p$ is the input vector, φ is a basis function, h is the smooth coefficient, c_j is the centroid of cluster j , ω_j is the weight and $\|\cdot\|$ is the Euclidean norm. We chose Gaussian form as the basis function by using following equation:

$$\phi(z) = \exp(-z^2). \quad (2)$$

We can construct a complete RBF network by determining the center position and the weights. To determine the center position, the objective function could be defined as follows

$$J_m = \sum_{i=1}^n \sum_{j=1}^k u_{ij} d_{ij}, \quad d_{ij} = \|\mathbf{x}_i - \mathbf{c}_j\|, \quad (3)$$

where x_i represent the i_{th} observation sample point, and u_{ij} can determine whether x_i belongs to the j_{th} membership function.

To minimize criterion J_m , namely $\min(J_m)$, an iteration algorithm is implemented by the following steps:

- (1) Randomly initialize the c-partition matrix according to

$$\sum_{i=1}^c u_{ij} = 1, \forall j = 1, \dots, N \quad (4)$$

and generate $U^{(0)}$.

- (2) Calculate the centroids of clusters by using

$$c_j = \frac{\sum_{i=1}^N u_{ij}^m \cdot x_i}{\sum_{i=1}^N u_{ij}^m}. \quad (5)$$

- (3) Compute the dissimilarity between centroids and data points by

$$u_{ij} = \frac{1}{\sum_{k=1}^c \left(\frac{\|x_i - c_j\|}{\|x_i - c_k\|} \right)^{\frac{2}{m-1}}}. \quad (6)$$

- (4) Stop iteration when

$$\|U^{(k+1)} - U^{(k)}\| \leq \varepsilon. \quad (7)$$

- (5) Update $U^{(k)}$ and go to Step (2).

- (6) Construct a k-dimension space vector

$$\mathbf{y}_i = \begin{bmatrix} \exp\left(-\frac{\|\mathbf{x}_i - \mathbf{c}_1\|^2}{h^2}\right) \\ \vdots \\ \exp\left(-\frac{\|\mathbf{x}_i - \mathbf{c}_k\|^2}{h^2}\right) \end{bmatrix}, \quad (8)$$

where the variances are identified, and

$$g(x_i) = \boldsymbol{\omega}^T \mathbf{y}. \quad (9)$$

(7) By implementing the least mean square error (LMSE) method, the matrix of the weight can be estimated as follows:

$$\hat{\boldsymbol{\omega}} = \begin{bmatrix} \hat{\omega}_{11} & \hat{\omega}_{12} & \cdots & \hat{\omega}_{1N} \\ \hat{\omega}_{21} & \hat{\omega}_{22} & \cdots & \hat{\omega}_{2N} \\ \vdots & \vdots & \vdots & \vdots \\ \hat{\omega}_{k1} & \hat{\omega}_{k2} & \cdots & \hat{\omega}_{kN} \end{bmatrix}. \quad (10)$$

3. FARX Model

3.1. Structure of ARX

Consider a single-input-single-output nonlinear system that can be configured as the following fuzzy relational equations:

$$\begin{aligned} \underline{R}^1 : \text{IF } x \text{ is } \underline{A}^1, \text{ THEN } y \text{ is } \underline{B}^1 \\ \vdots \end{aligned} \quad (11)$$

$$\underline{R}^r : \text{IF } x \text{ is } \underline{A}^r, \text{ THEN } y \text{ is } \underline{B}^r$$

The system could be described by a system of disjunctive rules, and we could decompose these rules into a single aggregated fuzzy relational equation as follows:

$$\begin{aligned} y = (x \circ \underline{R}^1) \text{AND} (x \circ \underline{R}^2) \text{AND} \\ \cdots \text{AND} (x \circ \underline{R}^r) \end{aligned} \quad (12)$$

or

$$y = x \circ \underline{R}$$

where, $\underline{R} = \underline{R}^1 \cap \cdots \cap \underline{R}^r$.

The ARX model could be incorporated into fuzzy relational equations. The FARX model could be written as the following equations:

$$\begin{aligned} \underline{B}^1 : \text{IF } y(t-1) \text{ is } \underline{B}^1, \text{ THEN } y(t) = -a_1^1 y(t-1) - \cdots - a_{n_a}^1 y(t-n_a) \\ + b_1^1 u(t-1) + \cdots + b_{n_b}^1 u(t-n_b) + e^1(t) \\ \vdots \\ \underline{B}^n : \text{IF } y(t-1) \text{ is } \underline{B}^n, \text{ THEN } y(t) = -a_1^n y(t-1) - \cdots - a_{n_a}^n y(t-n_a) \\ + b_1^n u(t-1) + \cdots + b_{n_b}^n u(t-n_b) + e^n(t) \end{aligned} \quad (13)$$

Above equations can be represented in an aggregated fuzzy relational equation as follows

$$y(t) = \underline{\mathbf{B}}^T(y(t-1)) \Theta \boldsymbol{\varphi}(t) + e(t), \quad (14)$$

where

$$\boldsymbol{\varphi}(t) = [y(t-1), \dots, y(t-n_a), u(t-1), \dots, u(t-n_b)]^T,$$

$$\Theta = \begin{bmatrix} a_1^1, \dots, a_{n_a}^1, b_1^1, \dots, b_{n_b}^1 \\ \vdots \\ a_1^n, \dots, a_{n_a}^n, b_1^n, \dots, b_{n_b}^n \end{bmatrix} = \begin{bmatrix} \boldsymbol{\theta}^1 \\ \vdots \\ \boldsymbol{\theta}^n \end{bmatrix},$$

$$\underline{\mathbf{B}}(y(t-1)) = [\mu_{B^1}(y(t-1)), \dots, \mu_{B^n}(y(t-1))]^T.$$

Eq. (14) could then be simplified as follows:

$$y(t) = \boldsymbol{\varphi}^T(t) \underline{\boldsymbol{\theta}} + e(t) \quad (15)$$

where, $\underline{\boldsymbol{\theta}} = \underline{\mathbf{B}}^T(y(t-1)) \Theta$.

3.2. Fault Feature Extraction Approach

The fault feature extraction approach could be given as following steps:

(1) Define membership functions.

Five Gaussian membership functions were used to represent the output y as shown in Figure 2.

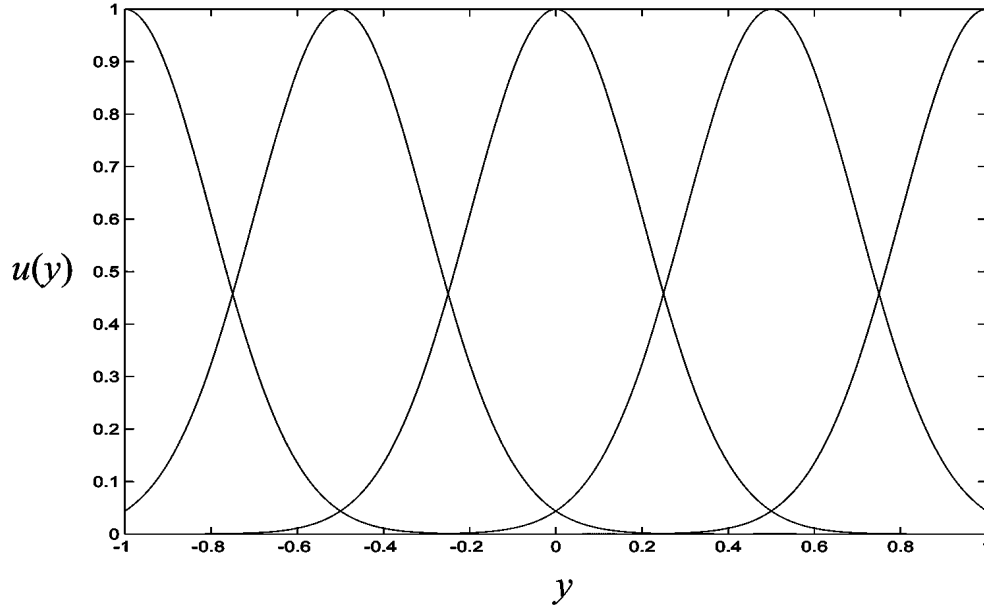


Figure 2. Membership Function of the Output y

(2) Define the fuzzy relational rules.

Fuzzy relational rules were consisted of five equations which can be given by

$$\begin{aligned}
 \mathcal{B}^1: & \text{ IF } y(t-1) \text{ is } \mathcal{B}^1, \text{ THEN } y(t) = -a_1^1 y(t-1) - \dots - a_{n_a}^1 y(t-n_a) \\
 & + b_1^1 u(t-1) + \dots + b_{n_b}^1 u(t-n_b) + e^1(t) \\
 & \vdots \\
 \mathcal{B}^5: & \text{ IF } y(t-1) \text{ is } \mathcal{B}^5, \text{ THEN } y(t) = -a_1^5 y(t-1) - \dots - a_{n_a}^5 y(t-n_a) \\
 & + b_1^5 u(t-1) + \dots + b_{n_b}^5 u(t-n_b) + e^5(t)
 \end{aligned} \tag{16}$$

(3) Establish the Fuzzy ARX model

We can establish a corresponding ARX model for each fuzzy rule. The parameters of the FARX model were estimated by applying the least square method:

$$\hat{\theta}^i = \left[\sum_{t=1}^N (\mu_{\mathcal{B}^i}(y(t-1)))^2 \boldsymbol{\varphi}(t) \boldsymbol{\varphi}^T(t) \right]^{-1} \sum_{t=1}^N \mu_{\mathcal{B}^i}(y(t-1)) \boldsymbol{\varphi}(t) y(t), \tag{17}$$

and

$$\hat{\boldsymbol{\theta}} = \begin{bmatrix} \hat{\boldsymbol{\theta}}^1 \\ \vdots \\ \hat{\boldsymbol{\theta}}^5 \end{bmatrix}. \tag{18}$$

(4) Extract the fault feature vector

The dimension of the parameter matrix was large; thus, the fault classifier could not properly determine the fault condition. To improve the efficiency of the fault diagnosis, we used the weighted vector as the fault feature vector:

$$\mathbf{f} = \lambda_1 \hat{\boldsymbol{\theta}}^1 + \dots + \lambda_5 \hat{\boldsymbol{\theta}}^5, \tag{19}$$

where $\lambda_1 + \dots + \lambda_5 = 1$.

4. Fault Diagnosis

First, samples of N target faults and a test fault were collected at a certain sample frequency. These sample data were then preprocessed to satisfy the requirement of the FARX model. The FARX models for each fault were established.

Second, the fault feature vectors were extracted according to Eq. (18). Considering N types of target faults, a dataset composed of N eigenvalue vectors could be obtained as follows:

$$\mathbf{F} = \begin{bmatrix} \boldsymbol{\theta}_1^T \\ \boldsymbol{\theta}_2^T \\ \vdots \\ \boldsymbol{\theta}_N^T \end{bmatrix}^T. \tag{20}$$

To determine the condition of a test fault, the eigenvalue vector of a test fault was incorporated into the dataset above to generate a new dataset:

$$\mathbf{F}_{new} = \begin{bmatrix} \boldsymbol{\theta}_1^T \\ \boldsymbol{\theta}_2^T \\ \vdots \\ \boldsymbol{\theta}_N^T \\ \boldsymbol{\theta}_{N+1}^T \end{bmatrix}^T. \tag{21}$$

The target fault dataset were used to train an RBF network classifier, and the output of the classifier was the result of the fault diagnosis. The complete fault diagnosis scheme based on RBF networks is shown in Figure 3.

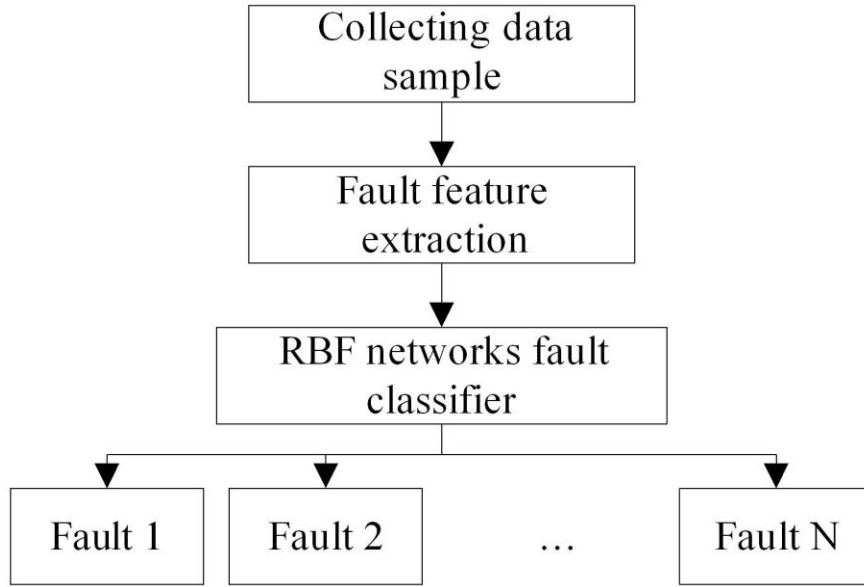


Figure 3. Fault Diagnosis Scheme based on RBF Networks

- (1) Training of the RBF network
 - 1) Initialize parameters and construct N discriminants $g_1(x), g_2(x), \dots, g_N(x)$;
 - 2) Calculate k centroids $\mathbf{c}_1, \mathbf{c}_2, \dots, \mathbf{c}_k$ by using $\mathbf{U}^{(r)}$;
 - 3) Compute n k-dimension $\mathbf{y}_1, \mathbf{y}_2, \dots, \mathbf{y}_n$ and carry fault feature vectors $\boldsymbol{\theta}_1, \boldsymbol{\theta}_2, \dots, \boldsymbol{\theta}_N$ and centroids $\mathbf{c}_1, \mathbf{c}_2, \dots, \mathbf{c}_k$ into the basis function;
 - 4) Estimate weight matrix $\hat{\boldsymbol{\omega}} \in R^{(k+1) \times N}$ by LMSE, and obtain an RBF network classifier.
- (2) Classification of the test fault sample
 - 1) Obtain $g_1(\boldsymbol{\theta}_f^{test}), g_2(\boldsymbol{\theta}_f^{test}), \dots, g_N(\boldsymbol{\theta}_f^{test})$ according to Eq. (13).
 - 2) If $g_i(\boldsymbol{\theta}_f^{test}) = \max(g_1(\boldsymbol{\theta}_f^{test}), g_2(\boldsymbol{\theta}_f^{test}), \dots, g_N(\boldsymbol{\theta}_f^{test}))$, we can determine that the test fault sample is the i fault; otherwise, we cannot determine the fault type.

5. Experiment

In this section, a 1.7 ton excavator hydraulic system was developed as the experimental platform for testing the proposed fault diagnosis approach. This excavator was produced by Sunward Equipment Group (Figure 4).



Figure 4. Experimental Platform of the 1.7 Ton Excavator

This experimental excavator consists of a boom, stick, and bucket and moves via tracks or wheels. The motion of the boom, stick, and bucket are driven by corresponding hydraulic cylinders. A basic operating cycle involves a digging pass through the bank, a loaded swing to dump position, a dump into a haul truck, empty swing back to digging, and repositioning or spotting of the bucket at the face. To fulfill these complex operations, an excavator is usually equipped with various hydraulic components, including a variable pump, proportional valves and cylinders. The variable pump converts mechanical energy to hydraulic energy and proportional valves distribute hydraulic energy to cylinders to drive the boom, stick, and bucket. Hence, we can simplify the hydraulic system of an excavator to several similar basic hydraulic loops despite of the functional difference (Figure 5).

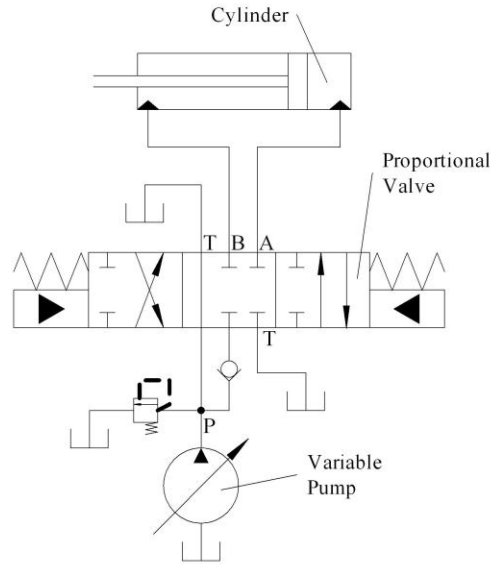


Figure 5. Basic Hydraulic Loop of the Excavator

By using the experimental excavator, the sample data was generated from three single fault cases including piston wear, spool stroke, and spool wear. The observation vector at time t , which was composed of variables from the simulation model, could be written as follows:

$$x(t) = [P_p(t), P_A(t), P_B(t), Q_p(t)]^T,$$

where P_p and Q_p are the pressure and the flow rate at pump outlet respectively. P_A and P_B are the pressure at port A and port B of valve respectively. The FARX model can be rewritten as follow

$$\begin{cases} Q_p(t) = FARX1(Q_p(t-1), Q_p(t-2), P_p(t-1), P_p(t-2)) \\ P_A(t) = FARX2(P_A(t-1), P_A(t-2), P_B(t-1), P_B(t-2)) \end{cases}$$

By using the experimental excavator, sample data was generated from three target fault cases:

- Fault 0: No faults
- Fault 1: Piston wear
- Fault 2: Spool stroke
- Fault 3: Spool wear

A case where more than one fault occurs simultaneously was not considered in this study. To obtain an adequate resolution for the hydraulic system, a 100Hz sample frequency could be used. The computation and analysis of the sample data were implemented in Matlab environment to verify the fault diagnosis approach.

Table 1. Target Fault Feature Vectors

| Fault type | Fault feature vector | | | | | | | | |
|------------|----------------------|--------|--------|--------|--------|--------|-------|--------|--|
| F0 | 4.249 | -0.536 | 1.421 | -2.504 | 5.271 | 0.731 | 0.537 | 0.256 | |
| F1 | 4.341 | -0.318 | 0.669 | -1.772 | -2.030 | 7.389 | 0.491 | -0.600 | |
| F2 | 4.187 | -0.440 | -0.619 | 0.286 | 6.099 | -0.798 | 0.105 | -0.152 | |
| F3 | 4.620 | -1.132 | 0.384 | -1.516 | 4.866 | 0.145 | 0.119 | -0.091 | |

Table 2. Fault Diagnosis Results based on RBF Network Classifier

| Test Fault Sample | Target Fault | | | | | | | | | result |
|-------------------|--------------|--------------|--------------|--------------|----------|----------|----------|----------|----------|--------|
| | $g_1(x)$ | $g_2(x)$ | $g_3(x)$ | $g_4(x)$ | $g_5(x)$ | $g_6(x)$ | $g_7(x)$ | $g_8(x)$ | $g_9(x)$ | |
| (1)F0 | 0.137 | 0.000 | 0.033 | -0.006 | 0.002 | 0.000 | 0.001 | 0.000 | -0.008 | F0(√) |
| (2)F1 | 0.000 | 0.120 | 0.000 | 0.000 | 0.000 | 0.000 | 0.000 | 0.000 | 0.000 | F1(√) |
| (3)F1 | 0.000 | 0.203 | 0.000 | 0.000 | 0.000 | 0.000 | 0.000 | 0.000 | 0.000 | F1(√) |
| (4)F2 | -0.015 | 0.000 | 0.591 | -0.043 | 0.013 | -0.059 | -0.001 | 0.000 | 0.026 | F2(√) |
| (5)F2 | -0.014 | 0.000 | 0.405 | -0.027 | 0.014 | -0.085 | -0.003 | 0.000 | 0.041 | F2(√) |
| (6)F3 | -0.004 | 0.000 | 0.047 | 0.599 | 0.083 | -0.029 | -0.015 | 0.000 | -0.061 | F3(√) |
| (7)F3 | -0.004 | 0.000 | 0.046 | 0.389 | 0.166 | -0.018 | -0.015 | 0.000 | -0.115 | F3(√) |

To avoid particular variables from inappropriately dominating the procedure, the training data should be normalized before developing a FARX model. The normalization consisted of two steps. The first step was to subtract the mean from each variable in the data. The second step was to divide each mean-centered variable by its standard deviation. This process scaled each variable in the sample data to zero mean and unit variance. Sample data should be scaled with the mean and variance vector of the normal condition sample data. We could extract fault feature vectors from model FARX1 and model FARX2 of Fault0, Fault1, Fault2 and Fault3 (Table 1).

Several test faults were introduced to verify the classification performance of the RBF network classifier. Fault feature vectors were used to train the RBF network classifier, and

then the RBF network classifier was used to classify the test fault. The classification result shows that all test faults were correctly classified (Table 2). The fault diagnosis by using RBF network classifier proves feasible and effective on the excavator hydraulic system.

6. Summary

A fault diagnosis approach by using RBF networks was proposed in this paper for hydraulic system. FARX models were developed by using sample data for target faults. Fault feature vector was extracted from the FARX models. RBF network classifier was used as the fault classifier to sort the test fault to the target faults. The hydraulic system of a 1.7 ton experimental excavator was developed to verify the fault diagnosis approach. Experiment results show that the proposed approach can be effectively applied to the fault diagnosis of the excavator hydraulic system.

Acknowledgements

This work is a project funded by the open foundation of the State Key Laboratory of Fluid Power Transmission and Control under Grant No. GZKF-201211, the Key Laboratory of Lightweight and Reliability Technology for Engineering Vehicle, Education Department of Hunan Province (Changsha University of Science & Technology) under Grant No. 2013KFJJ07 and the National Natural Science Foundation of China under Grant No. 51275059. The authors are would also like to express their sincerest gratitude to Ying Jiang for helpful discussions on this topic, and valuable comments on earlier drafts of this paper.

References

- [1]. M. Joorabian, S. M. A. Taleghani Asl and R. K. Aggarwal, "Accurate fault locator for EHV transmission lines based on radial basis function neural networks", *Electric Power Systems Research*, vol. 71, (2004), pp. 195-202.
- [2]. J. Park and J. W. Sandberg, "Universal approximation using radial basis functions network," *Neural Computation*, vol. 3, (1991), pp. 246-257.
- [3]. T. Poggio and F. Girosi, "Networks for approximation and learning," *Proc. IEEE*, vol. 78, (1990), pp. 1481-1497.
- [4]. S. Haykin, "Neural Networks: A comprehensive Foundation. Upper Saddle River", NJ: Prentice Hall, (1994).
- [5]. E. Ricci and R. Perfetti, "Improved pruning strategy for radial basis function networks with dynamic decay adjustment", *Neurocomputing*, vol. 69, (2006), pp. 1728-1732.
- [6]. H. Sarimveis, P. Doganis and A. Alexandridis, "A classification technique based on radial basis function neural networks" *Advances in Engineering Software*, vol. 37, (2006), pp. 218-221.
- [7]. J. M. Lattin, J. D. Carroll and P. E. Green, "Analyzing Multivariate Data", Beijing: Mechanical Industry Press, (2003).
- [8]. D. Zogg, E. Shafai and H. P. Geering, "Fault diagnosis for heat pumps with parameter identification and clustering", *Control Engineering Practice*, vol. 14, (2006), pp. 1435-1444.
- [9]. L. Ljung, "System Identification Theory for the User (2nd Edition)", Tsinghua University Press and Prentice Hall PTR, (2002).

Author



Xiangyu He, He received his master's and doctoral degrees in mechanical and electrical engineering and Ph. D. degree in Mechanical and Electrical Engineering from Central South University in 2000 and 2008, respectively. He is currently serving as a full time faculty in the College of Automobile and Mechanical Engineering, Changsha University of Science and Technology. His research interests include intelligent fault diagnosis methods and energy saving management.